On the structure of the boundary layer under adverse pressure gradient on an inclined plate

IOP Conf. Series: Journal of Physics: Conf. Series **1101** (2018) 012047 doi:10.1088/1742-6596/1101/1/012047

On the structure of the boundary layer under adverse pressure gradient on an inclined plate

V Uruba[1,2], P Procházka[1] and V Skála[1]

[1]Institute of Thermomechanics of the CAS, v. v. i., Dolejškova 5, Praha 8, Czech Republic
[2]University of West Bohemia, Faculty of Mechanical Engineering, Department of Power System Engineering, Universitní 8, Plzeň, Czech Republic
E-mail: uruba@it.cas.cz

Abstract. The presented study is focused on experimental investigation of a boundary layer on a flat plate in adverse pressure gradient. The flat plate is placed in regular flow, the pressure gradient is generated by the plate inclination. The study [9] deals with structure of the wake behind the plate, the presented study concentrates on structure of the flow close to the suction surface of the plate. Dynamical behaviour of the flow structures is studied in details with respect to the streamwise topology changes. In spite of the fact that the time-mean flow field is 2D, constant along the span, the instantaneous structures topology is fully 3D.

1. Introduction

The presented study is dedicated to experimental investigation of a boundary layer on a flat plate in adverse pressure gradient. The flat plate is placed in regular flow, the pressure gradient is generated by the plate inclination. The study [9] was focused on structure of the flow in the transversal planes, the presented paper studies the topology in streamwise direction close to the suction surface of the plate. In this region streamwise vortices emerge due to instability mechanism within the boundary layer subjected to adverse pressure gradient.

The presence of streamwise vorticity has been proved experimentally without any doubt – see e.g. [6, 7, 8]. The vortices are present in the suction region just above the plate, they touch the plate surface. However appearance of the vortices in this region is random both in space (position along the span) and time.

The aim of the present study is to get the relevant information about the topology of the vortices especially in the streamwise direction.

2. Experimental setup

Flat plate inclined with angle of attack (AOA) 7 degrees has been placed in a uniform low turbulent stream. The blow-down facility produces a jet with uniform velocity distribution, mean velocity about 5 m/s, intensity of turbulence less than 0.2%. The plate of thickness 2 mm has rounded edges, chord is 100 mm and span 450 mm. The Reynolds number based on plate chord is about 33 thousands. Schematics of the experiment is in figure 1.

The plane of measurement is located parallel to the plate surface in the distance from 2 up to 8 mm, defined as the constant Z value. The Cartesian coordinate system is introduced with X axis in streamwise direction parallel to the plate surface, Y in spanwise direction and Z perpendicular to the plate surface.

Origin of the coordinates is fixed on the upper plate surface at the centre of the leading edge (red dot in figure 1)

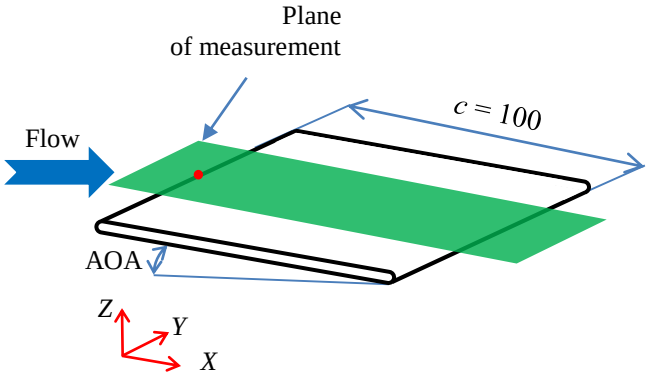

Figure 1. Schematics of the experiment.

3. Methods

The experimental methods and methods of data analysis will be described in details.

3.1. Instrumentation

The time-resolved PIV method was used for the experiments.

The measuring system DANTEC consists of the double-pulse laser with cylindrical optics and the CMOS camera. For the presented experiments the frequency was 2 kHz and 4000 double-snaps in sequence corresponding to 2 s of record for mean evaluation was acquired. The plane of measurement has been located parallel to the plate suction surface – see figure 1 in green. More details on measuring technique could be find in [8].

However the laser sheet thickness was approximately 1 mm, representing uncertainty of the measurement location. If the measuring plane is well defined in a distinct distance from the surface within the boundary layer viscous sublayer, then the value of the measured velocity is proportional to the local skin friction. The results should be considered as indicators only of the flow topology close to the surface, similar as results of surface flow visualisation using surface paintings. The vectorlines could be supposed to follow the skin friction on the surface.

More details on the near-wall PIV results interpretation see e.g. [1].

3.2. Analysis methods

The acquired velocity fields are to be subjected to further analysis. The classical statistical method are used for determining time mean and variances. Vorticity *Z*-component is evaluated as well. To demonstrate the dynamics of flow-field fluctuations topology the Proper Orthogonal Decomposition and Oscillation Pattern Decomposition methods are used.

The decomposition methods are based on idea Hilbert space, which is defined by the snapshots, forming the basis of the space. The goal of the decomposition methods is to find different, optimized basis with clear physical meaning.

The Proper Orthogonal Decomposition method (hereinafter POD) looks for the orthonormal modes basis maximizing the variance. Each mode consists of spatial pattern (Topos), evolution in time (Chronos) and amplitude, which is square root of kinetic energy (or enstrophy for vorticity) of the mode. The modes are ordered according to decreasing amplitude.

The POD method represents the classical approach to analyze the fluctuating flow topology on the basis of energetic content. Historically, it was introduced in the context of turbulence by Lumley [2] as an objective definition of what was previously called big eddies and which is now widely known as coherent structures.

The Oscillation Pattern Decomposition method (hereinafter OPD) evaluates the basis representing oscillating modes. The OPD method is based on stability assessment of fluctuation patterns in the flow under study. The method results into set of modes. Each mode is characterized by its frequency, damping factor called e-folding time and the topology. The periodical behavior is supposed with the given frequency and decaying amplitude, the mean time period for its decay by factor e is given by the e-folding time. Periodicity value is defined as the e-folding time to the mode period ratio, thus it is a dimensionless quantity. The mode topology is defined by a complex spatial mode. Its real and imaginary parts characterize fluctuating flow patterns shifted by a quarter of period, respectively.

More details on the OPD method could be find e.g. in [3,4,5].

4. Results

All presented results are given in dimensionless form, coordinates are divided by the plate chord defining the system (xyz). Velocities are divided by the inlet velocity U_e = 5 m/s defining dimensionless velocity components U and V. The OPD and POD modes are non-dimensional from definition.

The results evaluated in measuring planes in 4 distances from the suction plate surface z = 0.02, 0.04, 0.06 and 0.08, however detailed analysis will be shown for the measuring plane closest to the surface z = 0.02.

4.1. Statistics

Time mean flow-field will be shown first. In figures 2 and 3 the dimensionless streamwise mean velocity component U and sum of the dimensionless velocity components U and V variances sv distributions are shown respectively in the whole inspected domain. In figures 4 and 5 the same quantities are depicted within the single measuring plane z = 0.02. The spanwise mean velocity component V approaches zero value in the whole domain.

In figures 4 and 5 the lines x = 0 and x = 1 indicate positions of the leading and trailing edges respectively. In figures 2 and 4 the dark blue color indicates negative streamwise velocity component meaning back-flow region caused by the flow separation on the leading edge and reattachment close to the position x = 0.25. Above the separation zone there is a region of streamwise velocity overshoot, the velocity exceeds the free stream value (i.e. it is over 1).

The results indicate that the time-mean flow-field is more or less 2D, distributions are independent on the position y across the span.

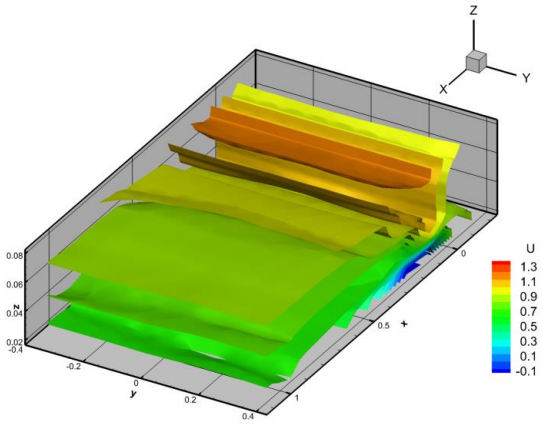

Figure 2. Iso-surfaces of dimensionless mean streamwise velocity component U.

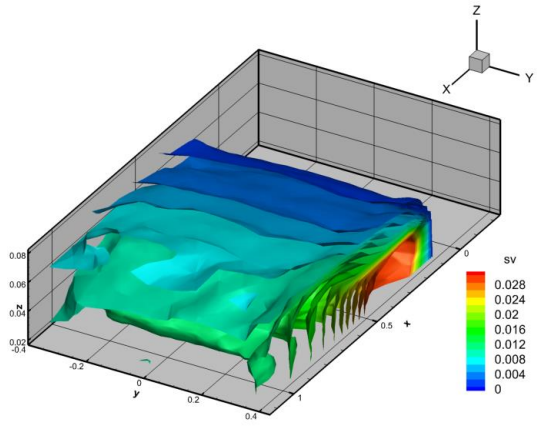

Figure 3. Iso-surfaces of sum of dimensionless velocity component variances sv.

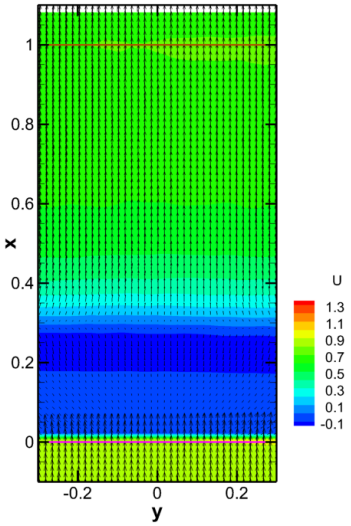

Figure 4. Dimensionless mean velocity *U* distribution.

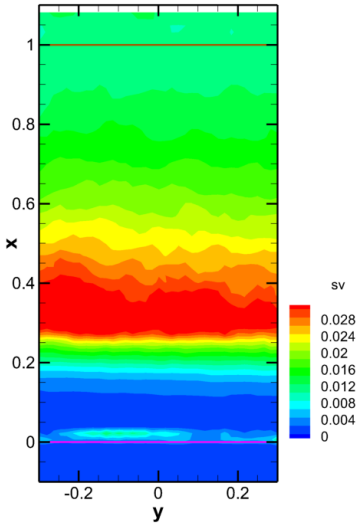

Figure 5. Sum of dimensionless velocity components variances *sv* distribution.

Maximal dynamical activity region is located just downstream the reattachment point – see the red color in figures 3 and 5.

For the subsequent dynamical analysis the domain was in the streamwise direction limited to the region with attached boundary layer $0.25 < x < 1$, i.e. between the reattachment point and the trailing edge.

4.2. OPD analysis of velocity fields

The OPD method has been applied on velocity vector distribution time-resolved data in the measuring plane $z = 0.02$, the 10 OPD modes has been evaluated.

Parameters of all OPD modes are given in table 1, in figure 6 there are the modes in the frequency – periodicity plain. The 3 modes no. 1, 5 and 8 with the largest value of periodicity were selected for presentation. Those modes are true oscillating ones represented by traveling patterns in the streamwise direction. The modes with low periodicity value or even 0 are of pulsating or decaying nature, not moving in space.

Table 1. OPD modes.

Mode	Frequency [Hz]	e-folding time [ms]	Periodicity [-]
1	104.0	23.3	2.42
2	61.8	22.3	1.38
3	34.8	22.2	0.77
4	29.9	21.6	0.64
5	117.5	21.2	2.49
6	42.6	20.6	0.88
7	76.6	17.7	1.36
8	133.0	15.2	2.02
9	0	14.8	0
10	0	12.0	0

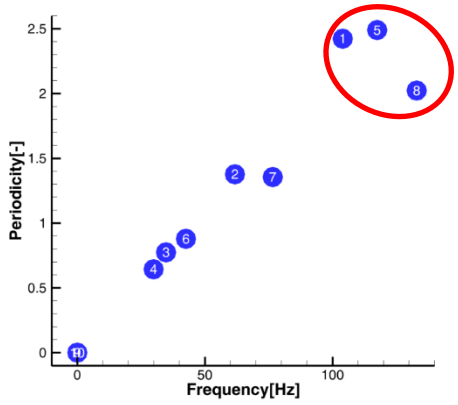

Figure 6. OPD spectrum, periodicity and frequencies of the OPD modes.

The spatial patterns will be shown for the selected modes, in figures 7 and 8 there are real and imaginary parts of the OPD mode 1 respectively. The mode topology is represented by the dimensionless velocity vector pattern and colour field representing dimensionless vorticity component perpendicular to the surface: red positive, blue negative values (the legend applies for figures 7 to 10).

The patterns in real and imaginary part of the OPD mode 1 are very similar, there is only difference in position of the patterns in streamwise direction and intensity. The intensity difference means that the amplitude of patterns changes periodically. The shift in space is connected with movement of patterns in the streamwise direction. Spacing of the structures is about 30 mm, divided by the mode period in time results in pattern velocity about 3 m/s, representing about 62% of incoming velocity.

For the OPD modes 5 and 8 only real parts of the topology will be shown in figures 9 and 10, the corresponding imaginary part is again shifted in *x* direction resulting in streamwise velocity of the pattern.

The studied OPD modes consist of shear layers, visible as vorticity concentration, in zigzag configuration.

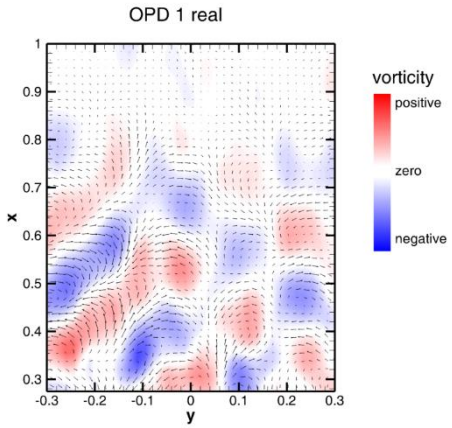

Figure 7. Real part of the OPD 1 mode.

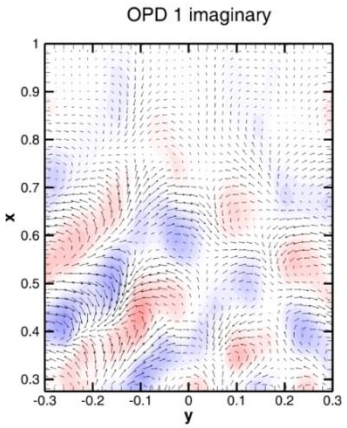

Figure 8. Imaginary part of the OPD 1 mode.

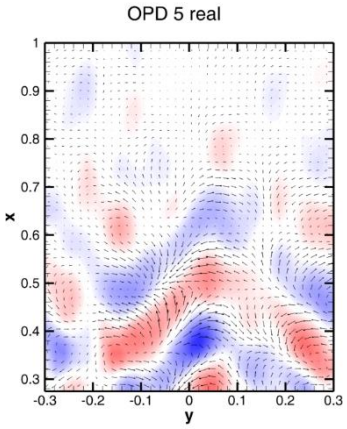

Figure 9. Real part of the OPD 5 mode.

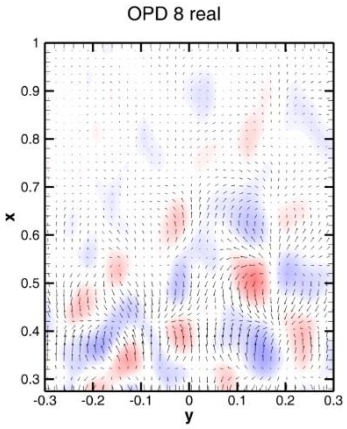

Figure 10. Real part of the OPD 8 mode.

4.3. POD analysis of vorticity fields

The vorticity *z*-component has been evaluated from all individual vector velocity fields. In figures 11 and 12 there is distribution of mean value and variance of vorticity, respectively. Mean vorticity forms streamwise streaks. Maximum of fluctuating activity is located just behind the reattachment, decaying in the streamwise direction.

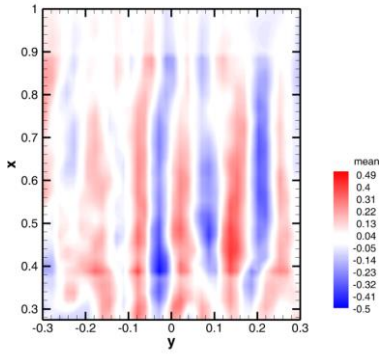

Figure 11. Mean dimensionless vorticity distribution.

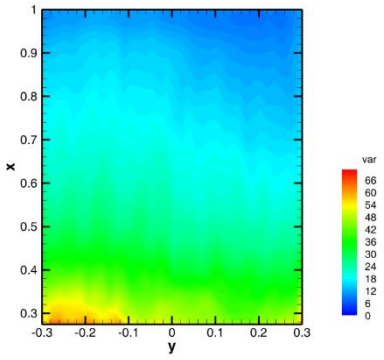

Figure 12. Dimensionless vorticity variance distribution.

The resulting vorticity fields have been subjected to the POD analysis to determine the modes explaining the vorticity variance, which could be considered as an enstrophy part. In figure 13 there is the enstrophy fraction and accumulated enstrophy of the vorticity POD modes depicted for all 2000 modes. The first POD mode contains 1.3% of the total enstrophy, while first 10 modes cover about 11%.

Selected POD modes topologies are to be shown. In figure 14 the Topos of the POD mode 1 is shown as vorticity fluctuations distribution (the legend apply for figures 6-18 as well). In figure 15 there is corresponding Topos representing time evolution of the mode 1, obtained as projection of the mode topology on the velocity vector field time series.

The higher order lower energy Toposes are shown in figure 16 number 4, in figure 17 number 40 and in figure 18 the POD mode number 99. The patters consist of vorticity strips in streamwise or oblique directions, filling the region behind the point of reattachment. Higher order modes fill the studied region regularly with smaller and more randomly distributed structures. The Topos representing time evolution

of the mode 99 is in figure 19. Comparing with time evolution of the mode 1 (figure 15), the presence of higher frequencies is visible.

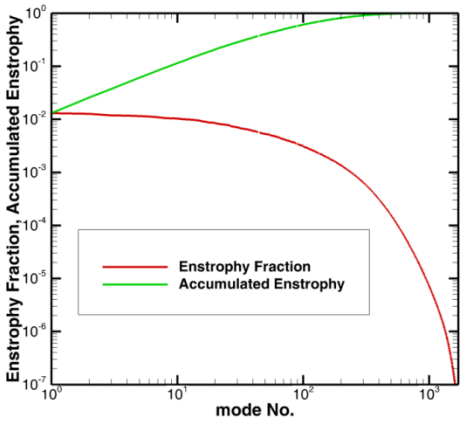

Figure 13. Enstrophy fraction and accumulated enstrophy of the vorticity POD modes.

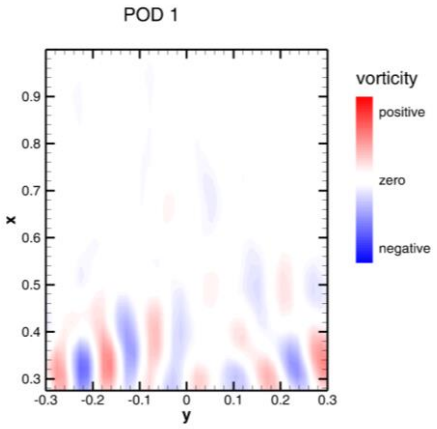

Figure 14. Topos of the POD 1 mode.

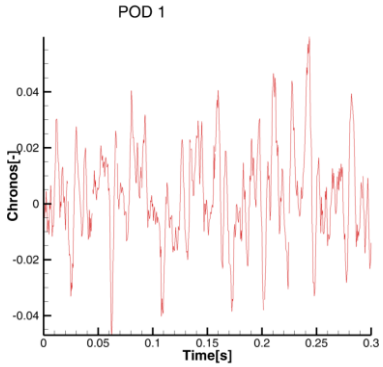

Figure 15. Chronos of the POD 1 mode.

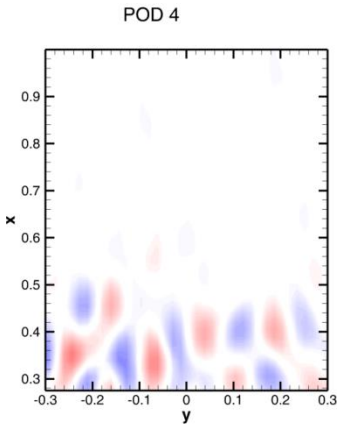

Figure 16. Topos of the POD 4 mode.

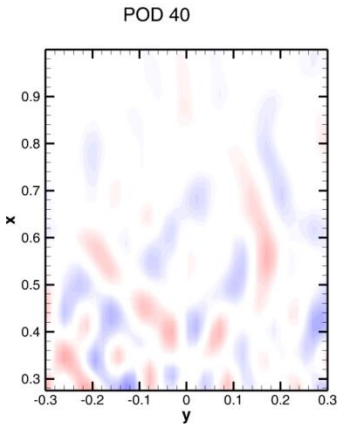

Figure 17. Topos of the POD 40 mode.

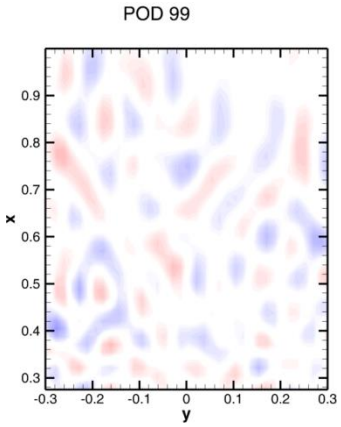

Figure 18. Topos of the POD 99 mode.

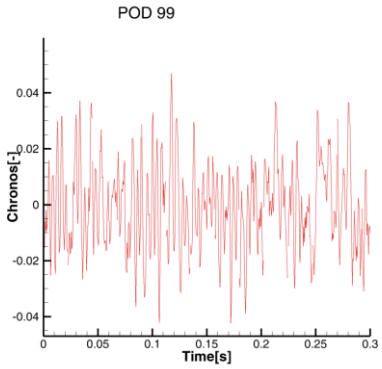

Figure 19. Chronos of the POD 99 mode.

5. Conclusions

Topology of the flow in the vicinity of suction surface of the flat plate in regular stream with angle of attack 7° was studied experimentally. Time resolved PIV method has been applied with measuring plane located close to the plate surface parallel to it. Local separation of the boundary layer has been detected on the first quarter of the surface. Both velocity and vorticity fields dynamics in the attached region have been explored in details. While the time-mean flow-field is close to 2D structure, the dynamical structures are highly 3D. Typical structures topology in the form of streamwise streaks and zigzag patterns have been shown. Maximal dynamical activity is located just behind the reattachment point decaying in the streamwise direction gradually.

Acknowledgements

This work was supported by the Grant Agency of the Czech Republic, project No. 17-01088S.

References

[1] Depardon, S., Lasserre, J.J., Boueilh J.C., Brizzi, L.E., Borée J., Skin friction pattern analysis using near-wall PIV, *Experiments in Fluids* **39**, 805–818, 2005.
[2] Lumley, J.L., The structure of inhomogeneous turbulent flows, Atm.Turb. and Radio Wave Prop., Yaglom and Tatarsky eds., Nauka, Moskva, pp. 166-178, 1967.
[3] Hasselmann, K., PIPs and POPs: The Reduction of Complex Dynamical Systems Using Principal Interaction and Oscillation Patterns, *Journal of Geophysical Research* **93**, D9, 11.015-11.021, 1988.
[4] Uruba, V., Decomposition Methods in Turbulence Research, *EPJ Web of Conferences* **25**, 01095, 2012.
[5] Uruba, V., Near wake dynamics around a vibrating airfoil by means of PIV and Oscillation Pattern Decomposition at Reynolds number of 65000, *Journal of Fluids and Structures* **55**, 372–383, 2015.
[6] Uruba, V., Pavlík, D., Procházka, P., Skála, V. and Kopecký, V., On 3D flow-structures behind an inclined plate, *EPJ Web of Conferences* **143**, 02137, 2017.
[7] Uruba, V., Pátek, Z., Procházka, P., Skála, V., Zacho, D. and Kulhánek, R., Flow Structure behind a Wing at High Reynolds Numbers, *EPJ Web of Conferences* **180**, 02111, 2018.
[8] Uruba, V., Procházka, P. and Skála V., On 3D Flow Structure of the Boundary Layer on the Suction Side of a Plate, *EPJ Web of Conferences* **180**, 02112, 2018.
[9] Uruba, V., Procházka, P. and Skála, V., On the 3D structure of the flow-field in the vicinity of inclined plate, to be published.